

ME 614 Spring 2017-Homework 2
Numerical Stability, Advection & Diffusion

Zitao He
3/10/2017

Problem 1.

The truncation errors with different precision(float16, float32, float64) are explored. The results are shown below:

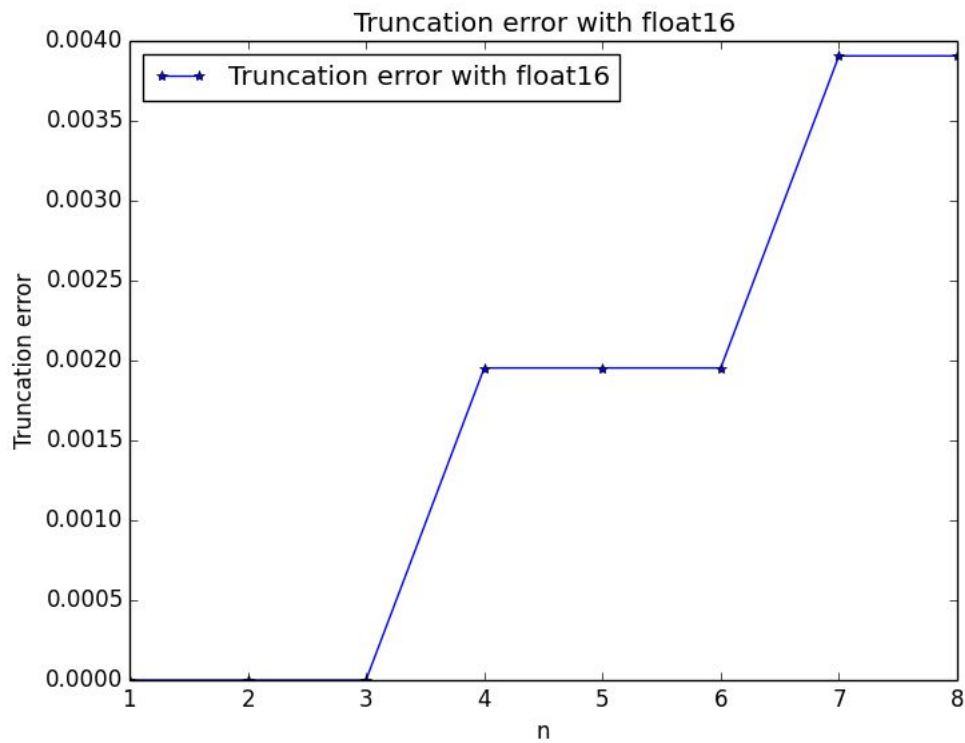


Figure 1. Truncation error with precision float16

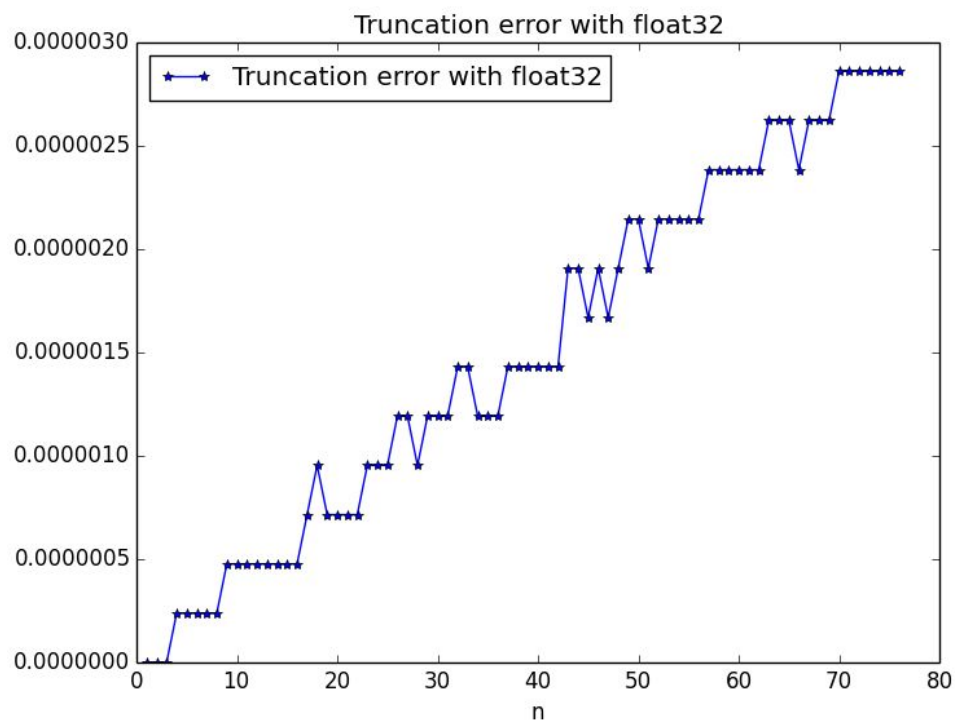


Figure 2. Truncation error with precision float32

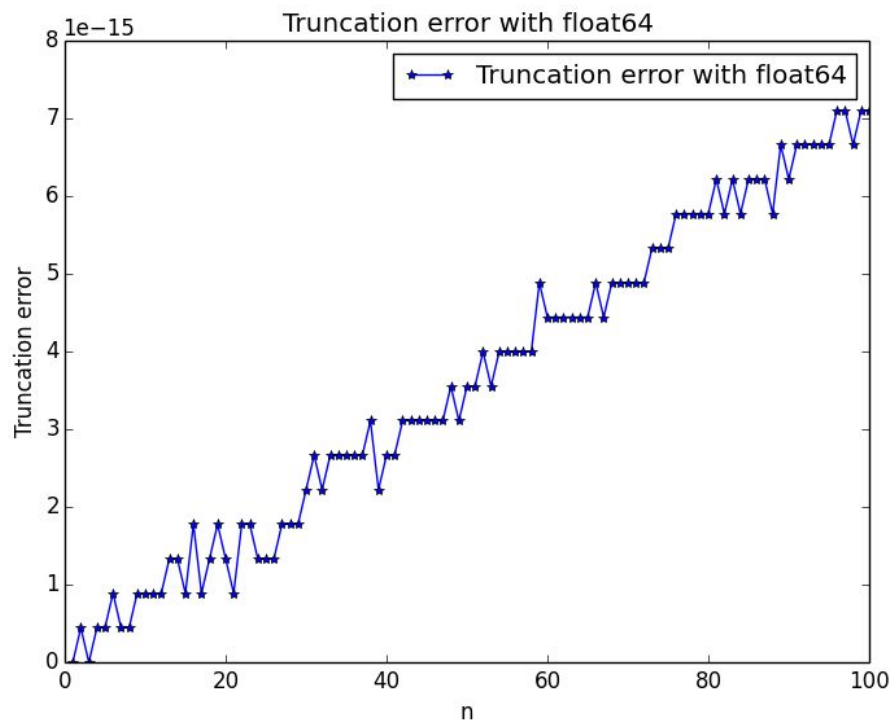


Figure 3. Truncation error with precision float64

As we can see. With n increases, the truncation error will increase because of round-off error accumulates. With higher precision (float 64), and the same n , the truncation error is smaller.

Problem 2.

In this part, the advection and diffusion PDE based on the periodic conditions is evaluated.

(a) From part (b), the analytical solution is used to evaluate the performance of different schemes and different spatial discretization. The analytical solution and numerical solution overlaps very well especially for very fine grid. This means the analytical function $u(x, t)$ satisfies the given PDE.

Also, we can verify that by hand:

$$u(x, t) = C_1 e^{-w_1^2 \alpha t} \sin[w_1(x - ct) - Y_1] + C_2 e^{-w_2^2 \alpha t} \cos[w_2(x - ct) - Y_2]$$
$$\frac{\partial u}{\partial t} = -C_1 w_1^2 \alpha e^{-w_1^2 \alpha t} \sin[w_1(x - ct) - Y_1] - C_1 C_1 w_1 e^{-w_1^2 \alpha t} \cos[w_1(x - ct) - Y_1]$$
$$+ C_2 w_2^2 \alpha e^{-w_2^2 \alpha t} \cos[w_2(x - ct) - Y_2] - C_2 C_2 w_2 e^{-w_2^2 \alpha t} \sin[w_2(x - ct) - Y_2]$$
$$\frac{\partial u}{\partial x} = w_1 C_1 e^{-w_1^2 \alpha t} \cos[w_1(x - ct) - Y_1] + w_2 C_2 e^{-w_2^2 \alpha t} \sin[w_2(x - ct) - Y_2]$$
$$\frac{\partial^2 u}{\partial x^2} = -w_1^2 C_1 e^{-w_1^2 \alpha t} \sin[w_1(x - ct) - Y_1] + w_2^2 C_2 e^{-w_2^2 \alpha t} \cos[w_2(x - ct) - Y_2]$$

It is clear that $\frac{\partial u}{\partial t} + c \frac{\partial u}{\partial x} - \alpha \frac{\partial^2 u}{\partial x^2} = 0$

(b) Given some constants, with different number points in domain($N = 10, 25, 50, 100$), solutions are plotted at time = T_f . The figures below show the results.

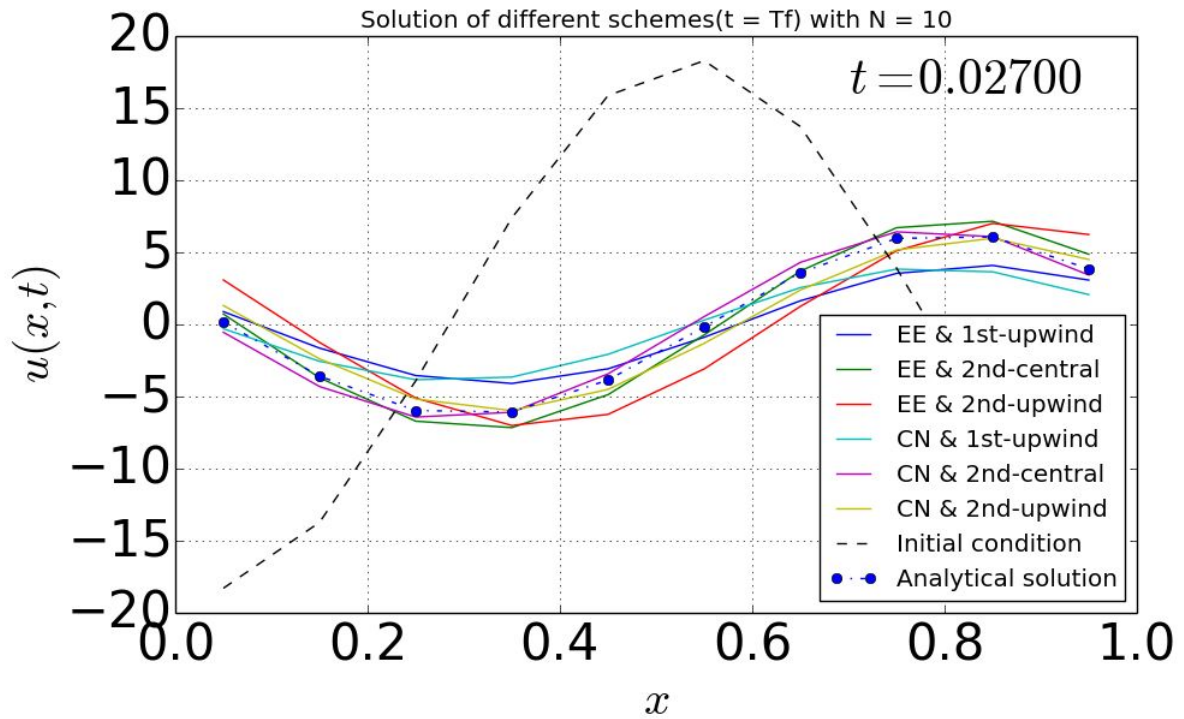


Figure 4. Solutions of different schemes with $N = 10$

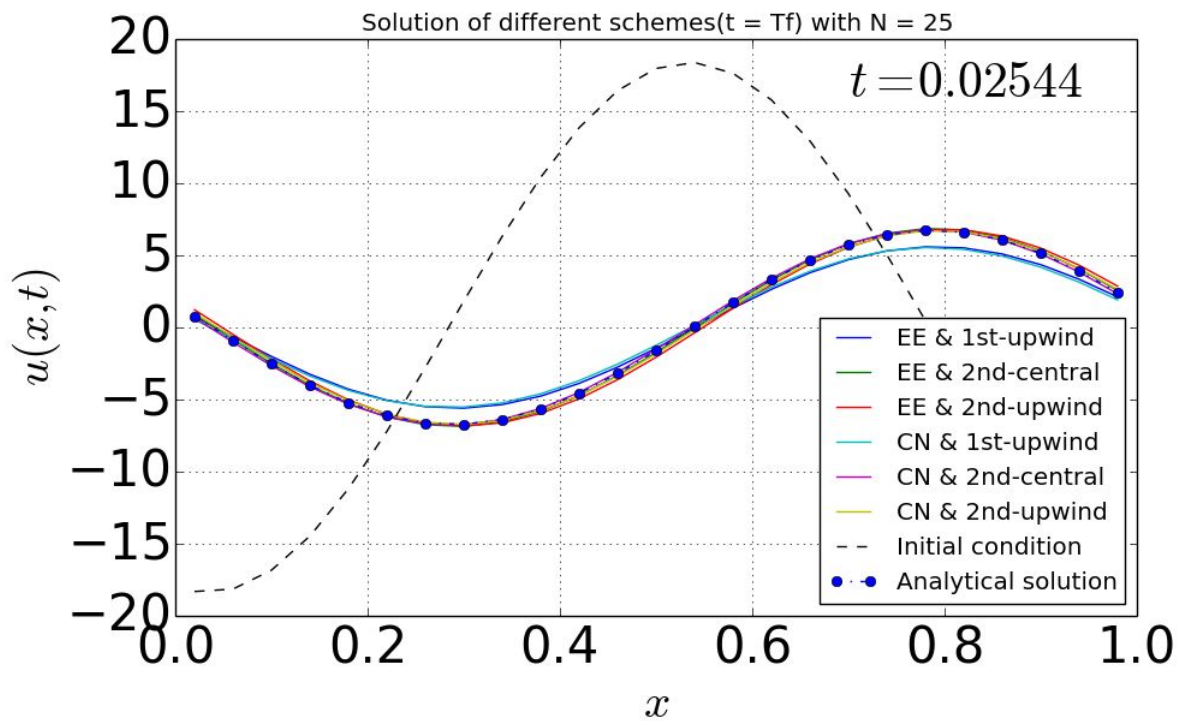


Figure 5. Solutions of different schemes with $N = 25$

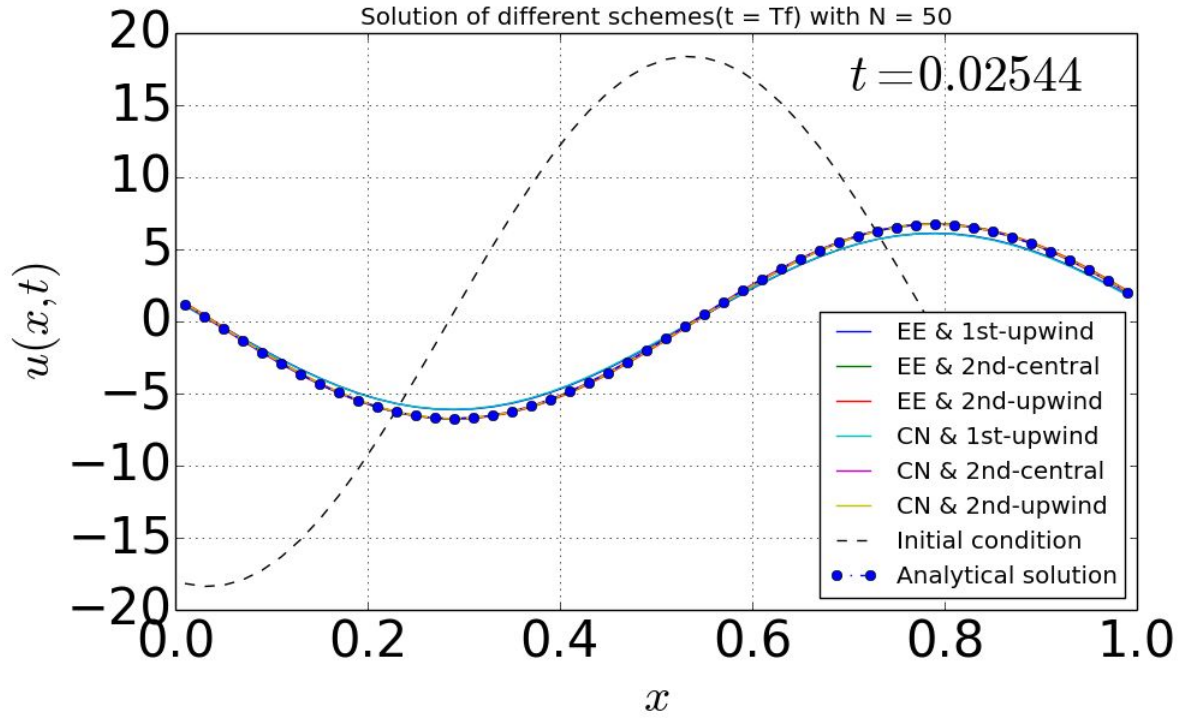


Figure 6. Solutions of different schemes with $N = 50$

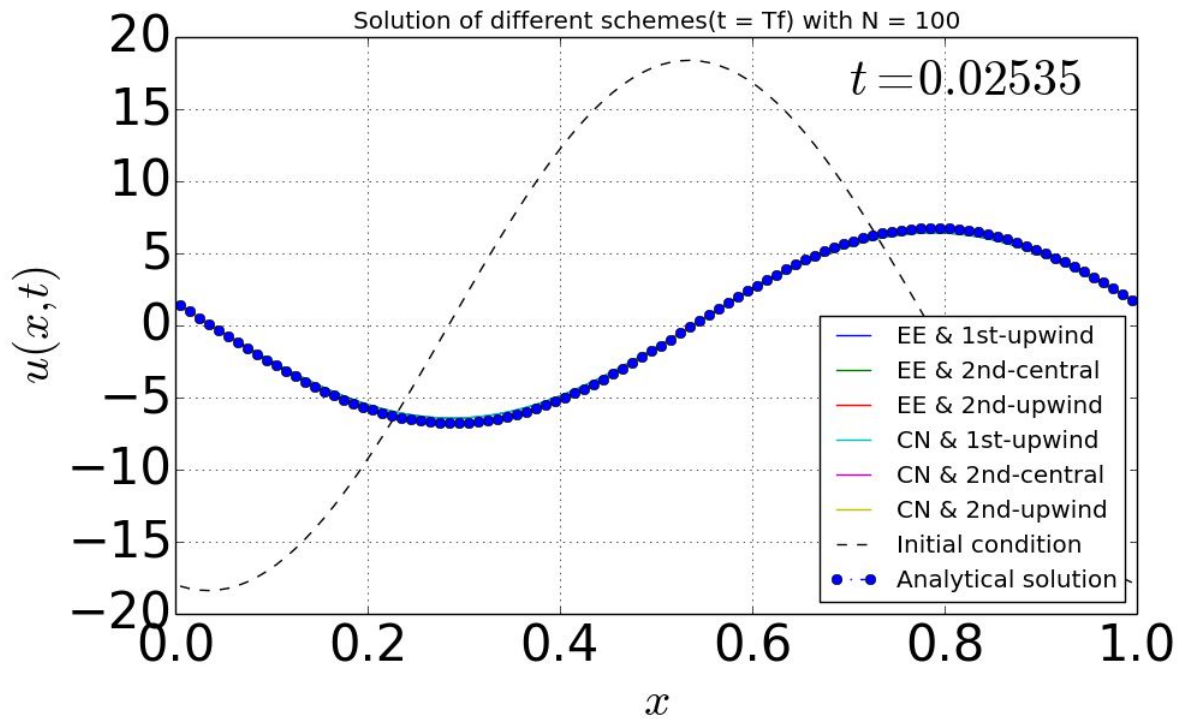


Figure 7. Solutions of different schemes with $N = 100$

As you can see, with increasing points(N), the solutions for six schemes are closer to the analytical solution which means finer grid will result more accurate numerical solutions. For $N = 10$, the best scheme seems to be Crank-Nicolson & 2nd-order-central scheme, and the worst scheme seems to be 1st-order-upwind scheme(both for Crank-Nicolson and Explicit Euler). But if the number of points keeps increasing, the difference between the best and worst scheme is not distinguishable anymore.

(c) For all of the aforementioned spatial discretizations but for the Crank-Nicholson time-advancement method only, root-mean-square error at constant Δt and constant Δt was plotted. The results are shown below.

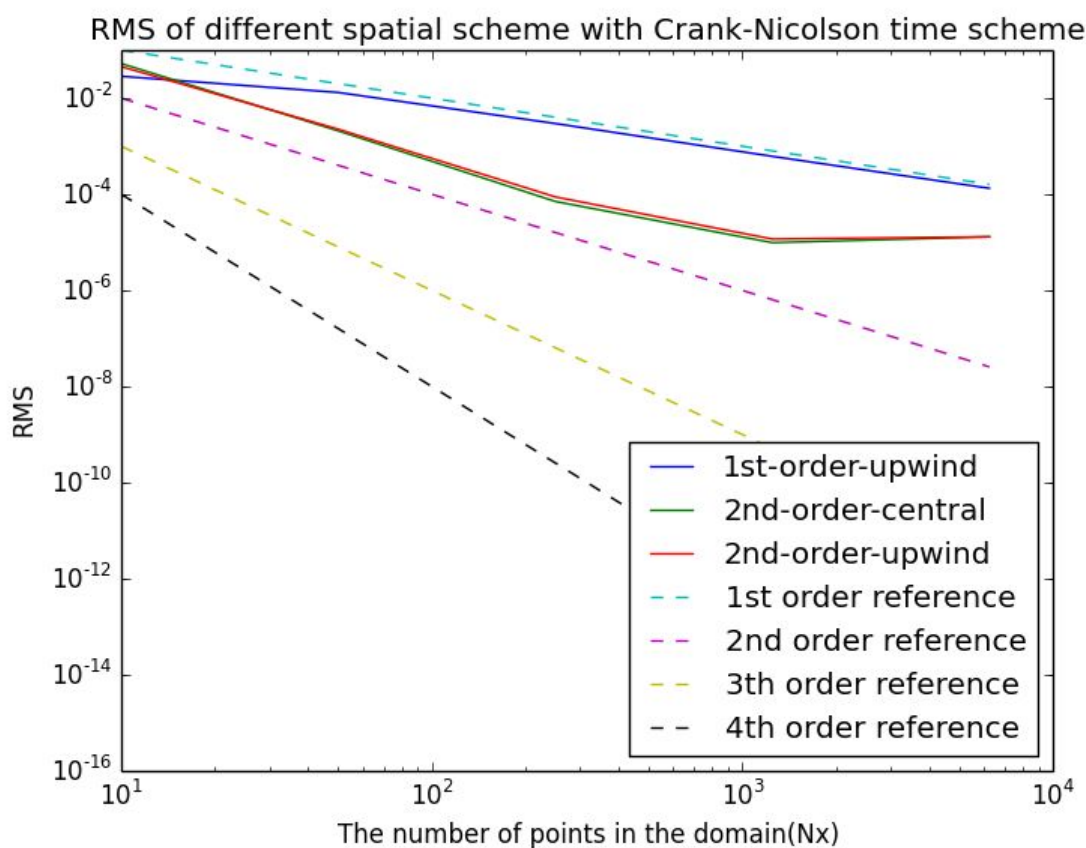


Figure 8. RMS for schemes with constant Δt

From the figure with constant Δt , it seems like the 1st-order scheme convergences with order of 1 and 2nd order scheme first convergence with order of 2 and then go flat. This is because with grid goes finer, RMS is not coming from the numerical method itself, instead, RMS now is mainly coming from round-off error. Since the RMS is an average value, the RMS with very fine grid will keep constant.

What's more, 2nd-order-central scheme and 2nd-order-upwind overlaps well. However, the curve of 2nd-order central scheme is slightly slower than the curve of 2nd-order upwind.

The reason can be explained by Prof. Scalco: **Second-order central is a better derivative than the upwind one (remember HW1). Upwind is more diffusive and more stable for calculations and better suited for low Reynolds number applications. Central is better for turbulent calculations.**

Also, the 2nd-order scheme goes to flat more quickly than 1st-order (there should be flat area for 1st order scheme when N is large enough). This is because 2nd-order schemes are, apparently, more stable than 1st-order scheme.

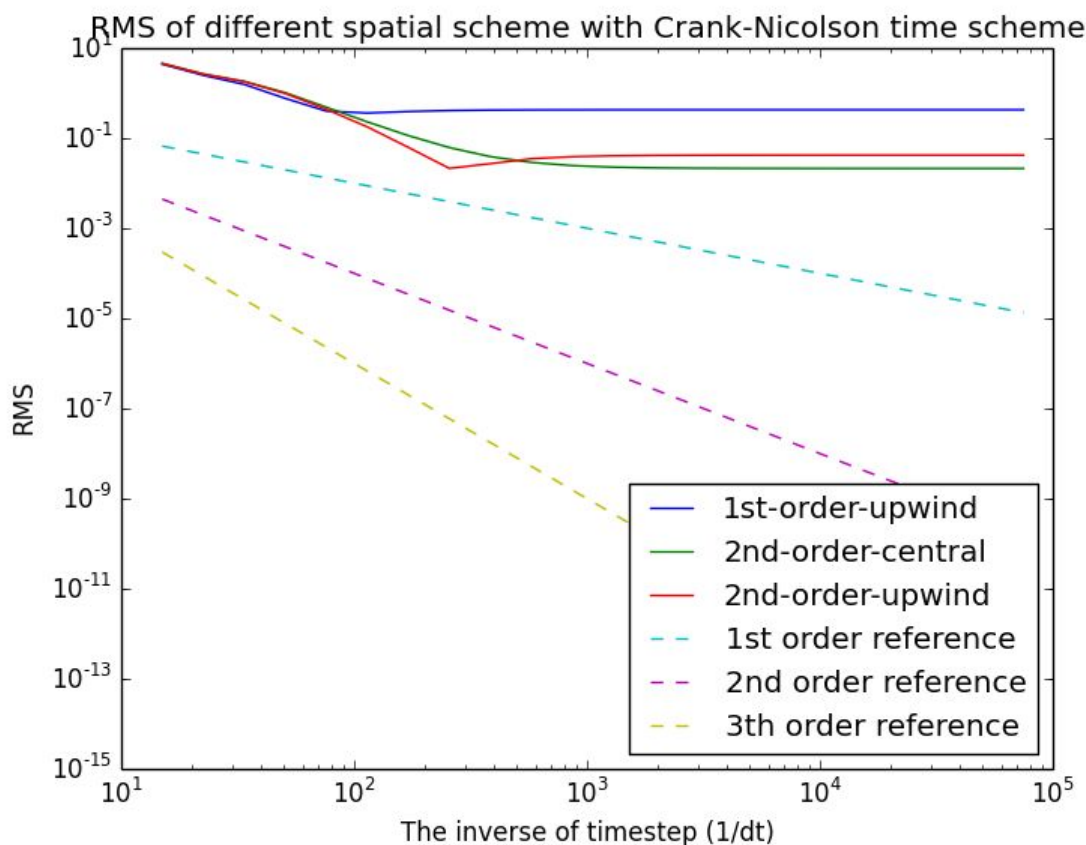
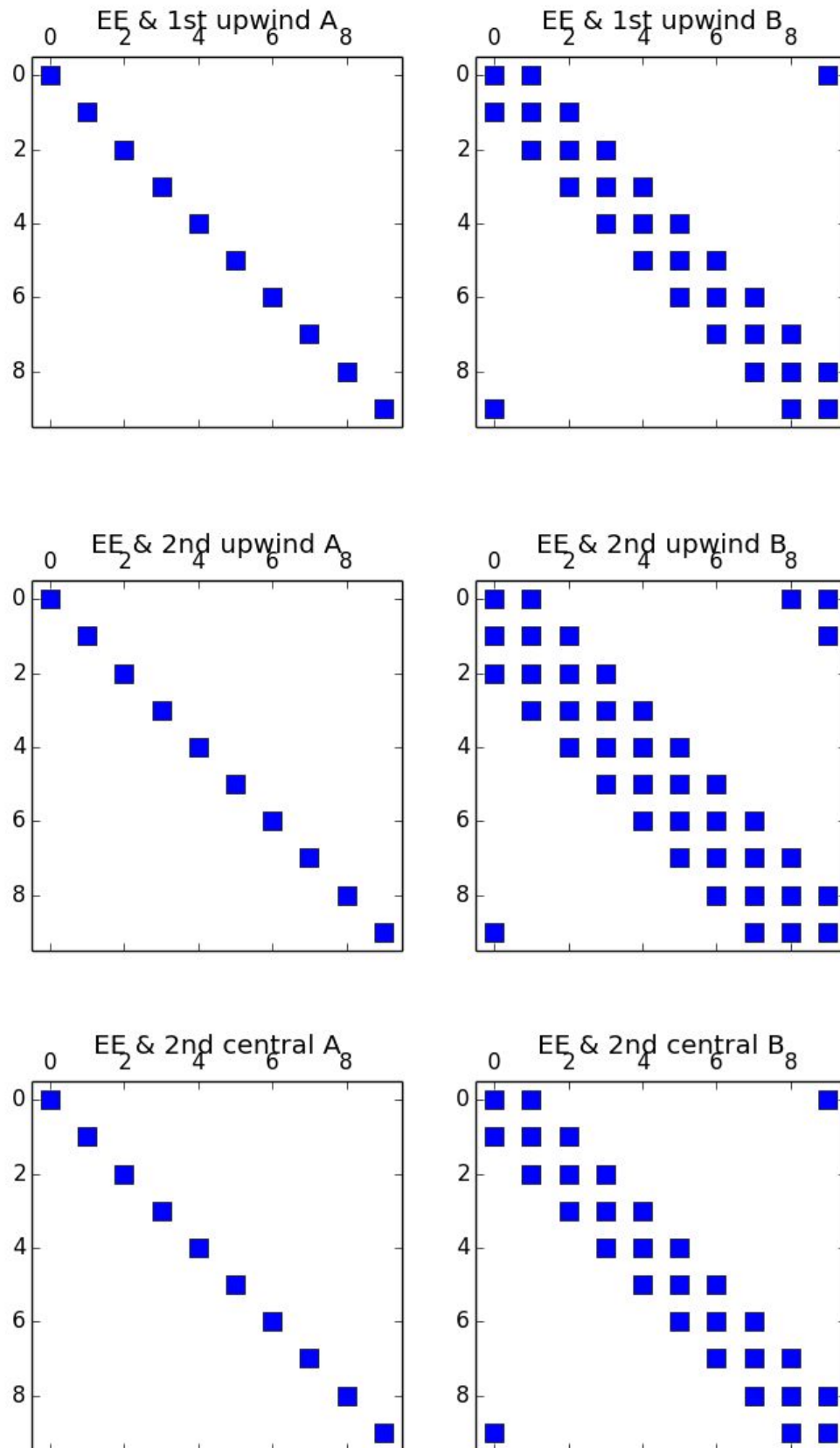
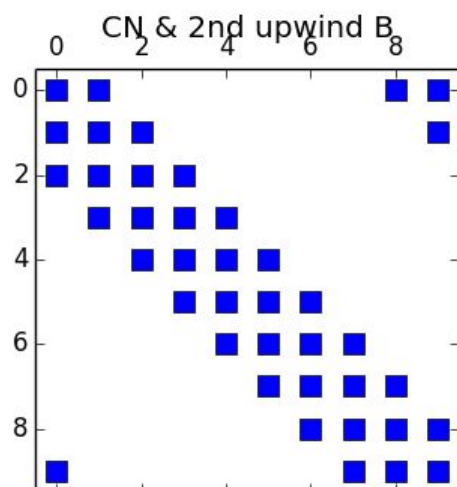
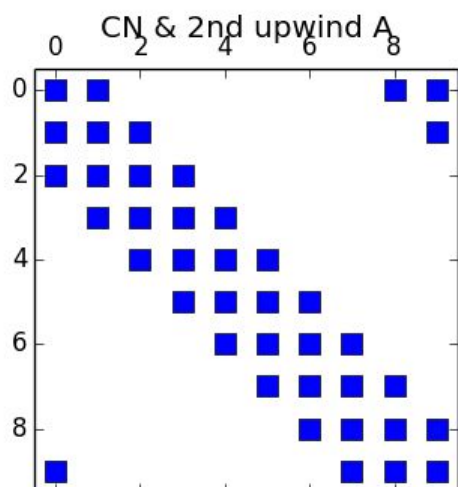
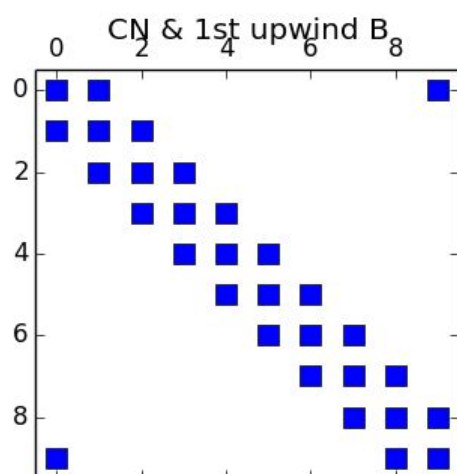
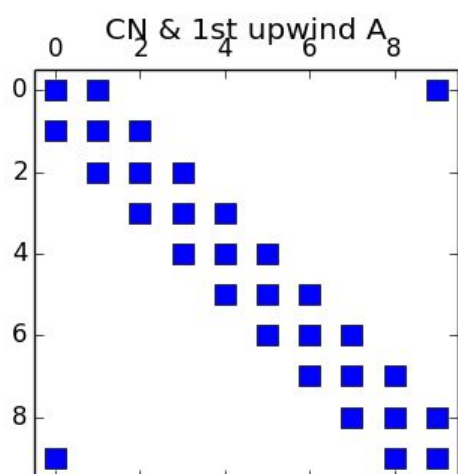


Figure 9. RMS for schemes with constant dx

With constant dx , things look similar as in figure with constant dt . However, the order of convergence is hard to determine. But I believe they should convergence with order of 2. The curve of different schemes are highly dependent on the parameters we set.

(d) The diagram of matrix A and B of different schemes are listed below





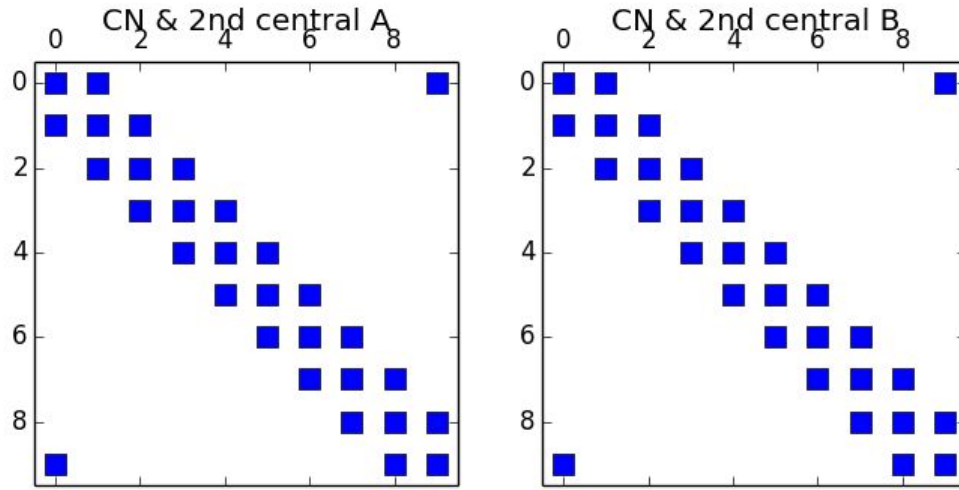


Figure 10. Diagram of matrix A and B for each scheme.

(e) For Explicit Euler scheme only, select the range of C_c and C_α ((0,2) and (0,5) respectively) and then calculate corresponding dt and dx and then calculate spectral radius of transition matrix T . Flooded iso-contours of the spectral radius of the transition matrix T were shown below:

If the solution is stable, the spectral radius of transition matrix must be smaller or equal to 1. The green areas for each figure represent the area where the spectral radius is exactly 1, so in result, represent stable area. Only in this area will the solution be stable.

As you can see, the stable area(green area) of central scheme is larger than upwind schemes (both for 1st-order and 2nd-order) which means that the central schemes are more stable than upwind schemes. This can also be demonstrated in the aforementioned figures (from the RMS figure with constant dx).

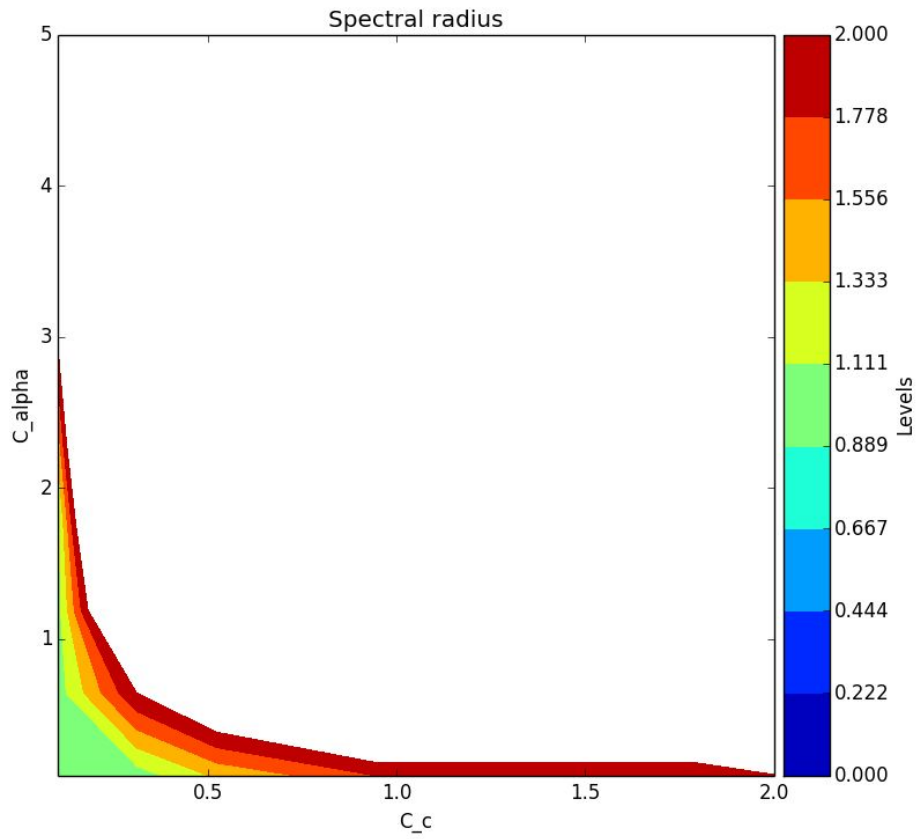


Figure 11. Spectral radius contour plot of Explicit Euler & 1st-order upwind

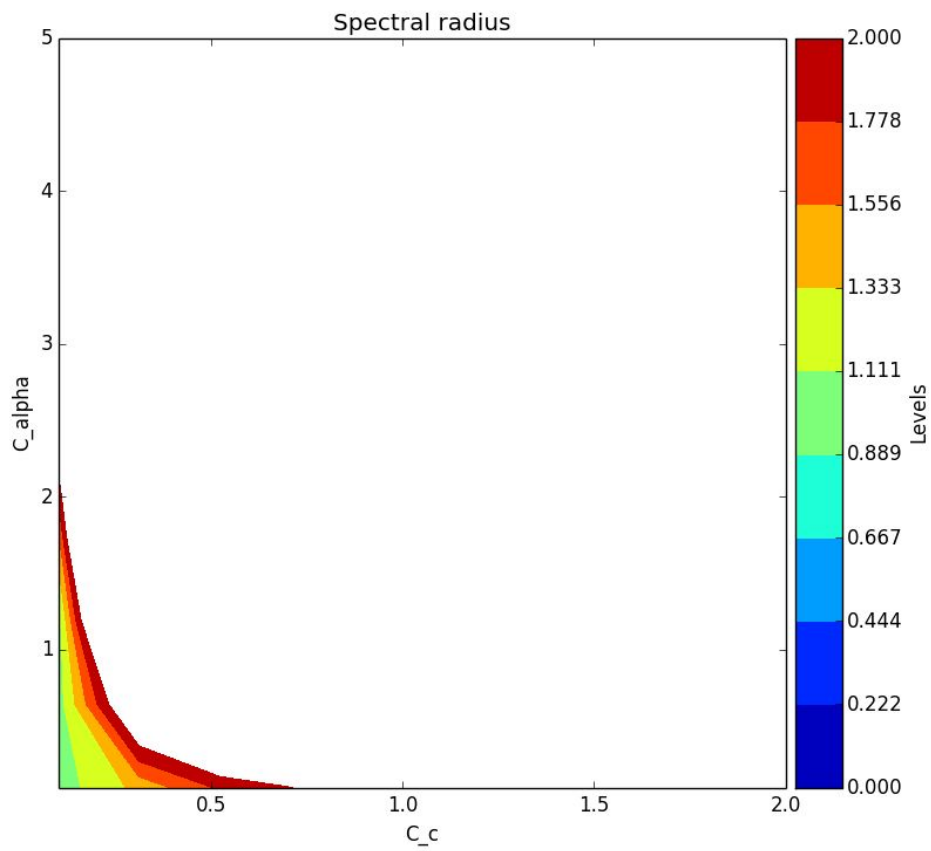


Figure 12. Spectral radius contour plot of Explicit Euler & 2nd-order upwind

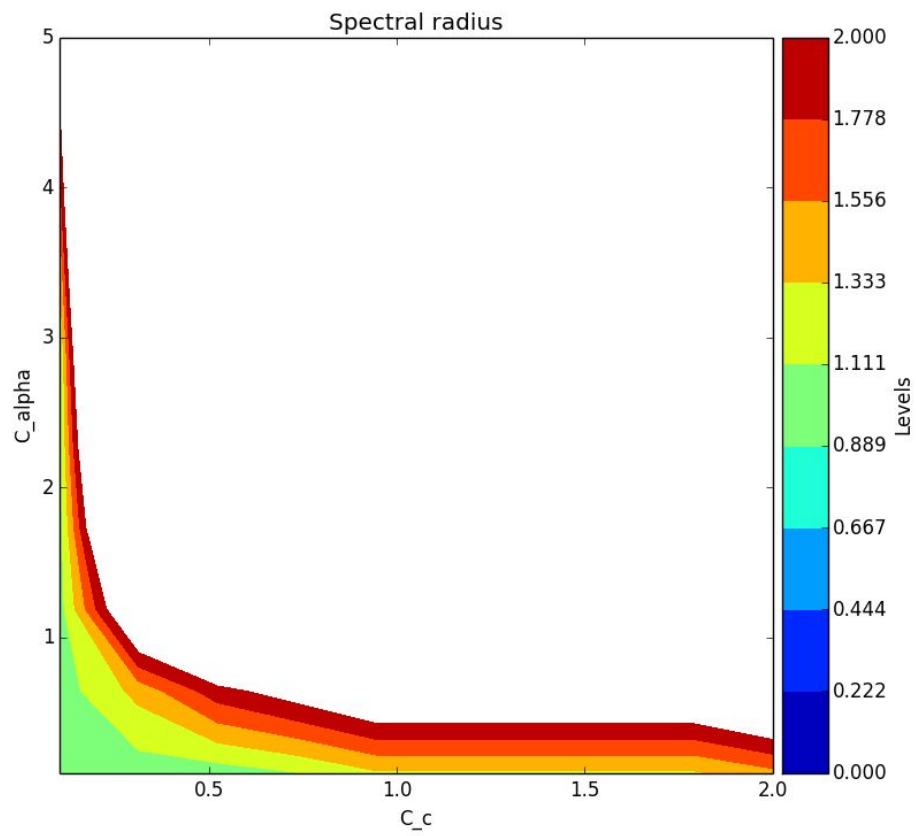


Figure 13. Spectral radius contour plot of Explicit Euler & 2nd-order central

Problem 3.

(a) Some parameters are changed and compared with reference steady-state solution to see the behavior of each parameters. The results are shown below:

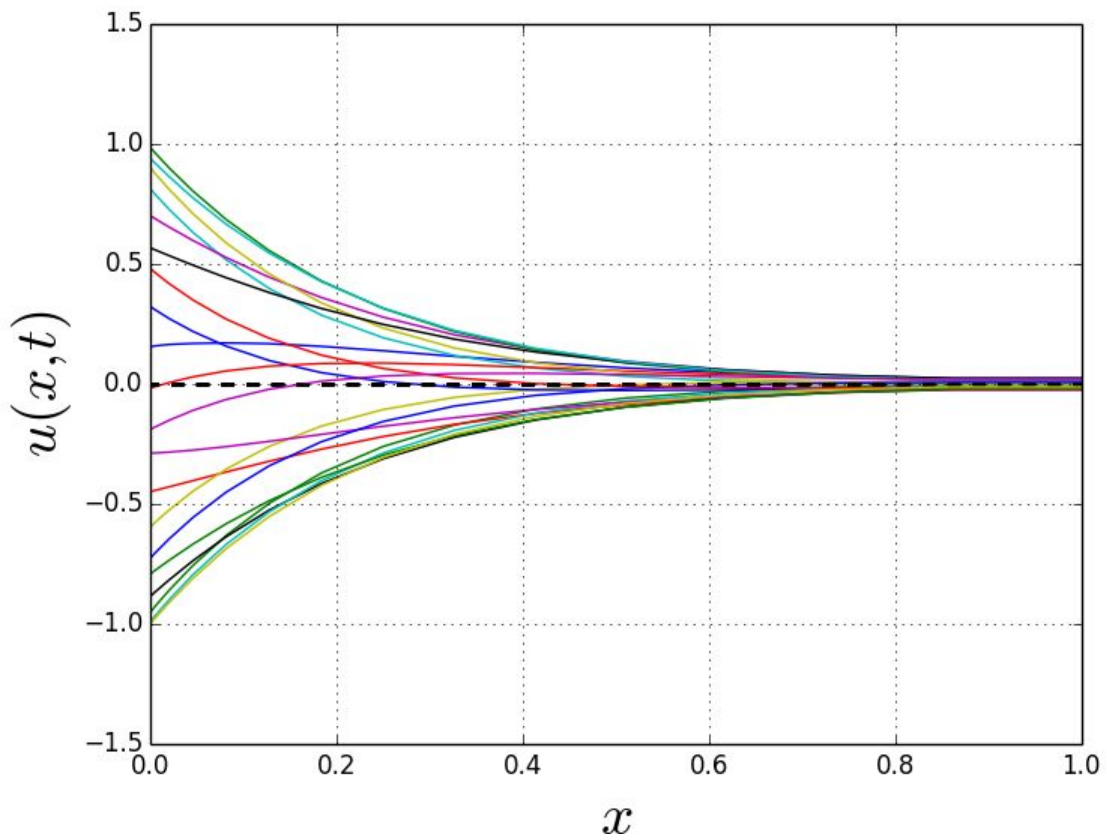


Figure 14. Reference steady-state solution

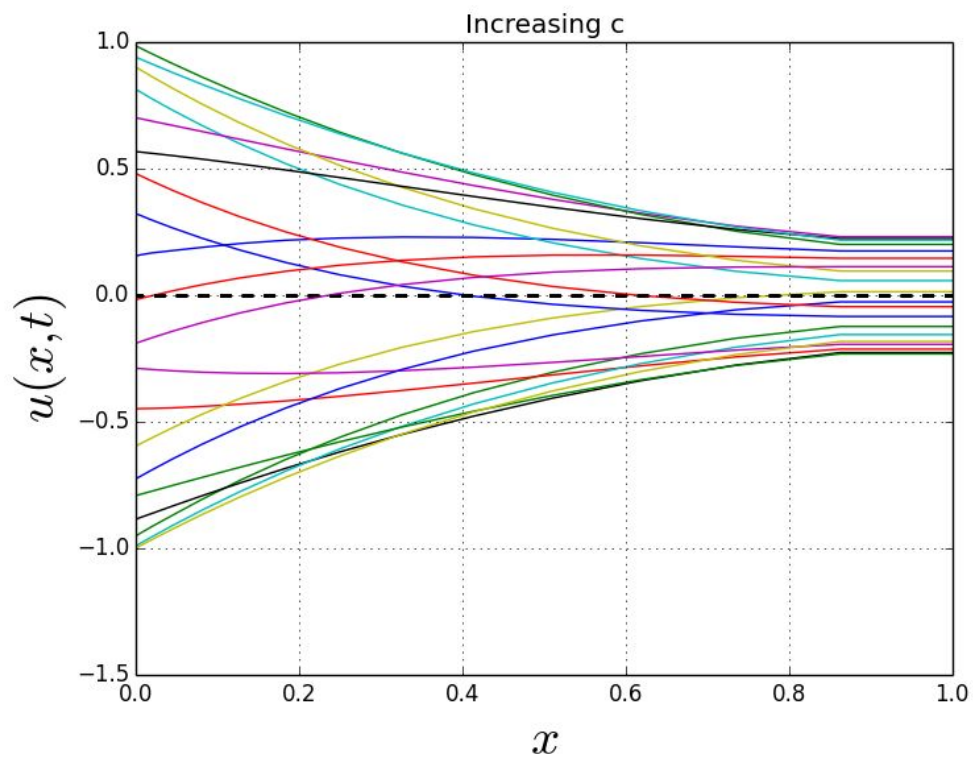


Figure 15. Steady-state solution with increasing c

With c increases, the advection speed will increase, and more uniform solution will be obtained.

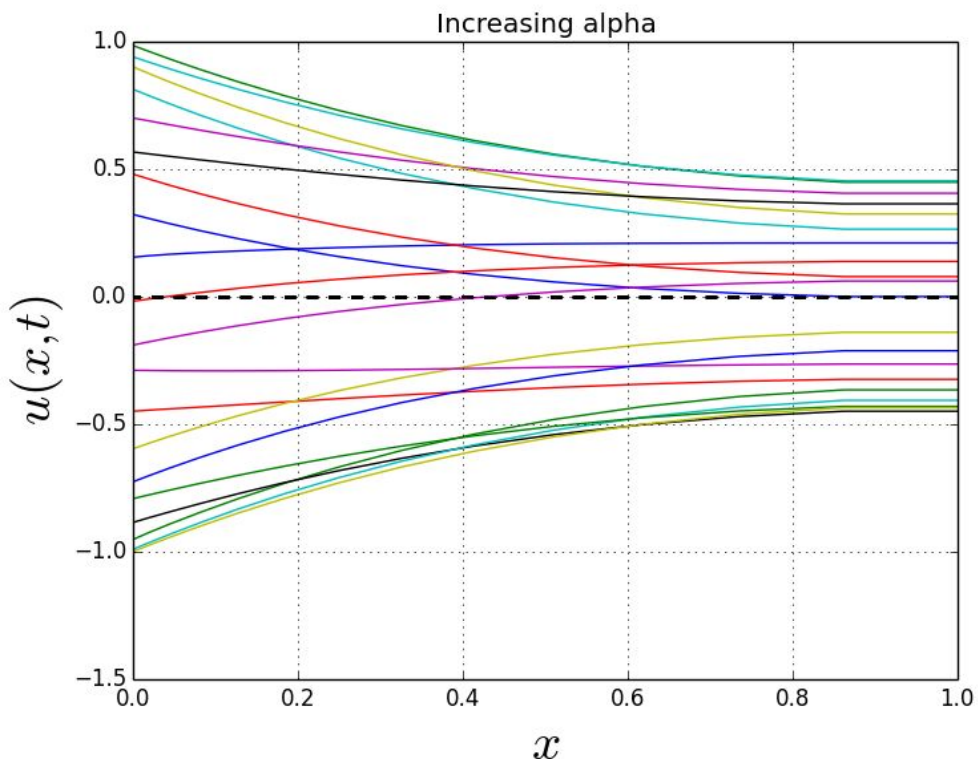


Figure 16. Steady-state solution with increasing alpha

With alpha increases, the diffusion behavior is stronger which will result in more uniform solution as well.

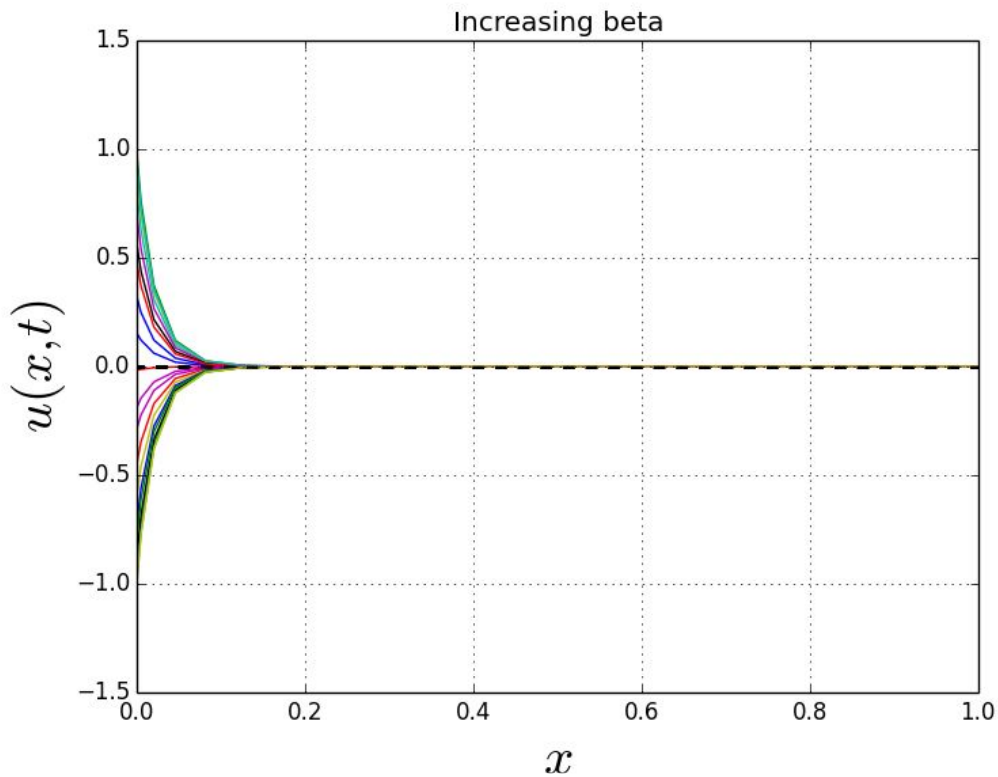


Figure 17. Steady-state solution with increasing beta

With beta increases, the solution convergences more easily to the initial condition (hard to change the value of u around x-axis).

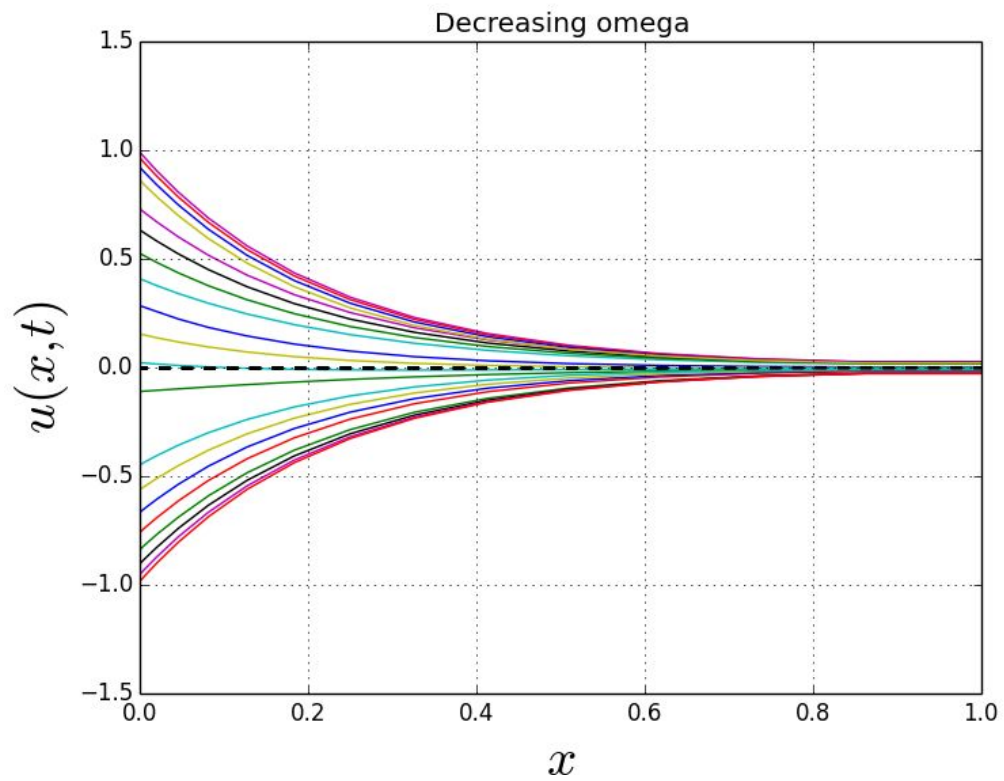


Figure 18. Steady-state solution with decreasing omega

With decreasing omega, the advection behavior of solution disappears. Only the diffusion behavior survived. This can be explained by: with low omega(frequency), the period of boundary condition T is relatively high and the boundary condition on the left moves very slowly. When the solution was plotted, the advection fluid is already gone.

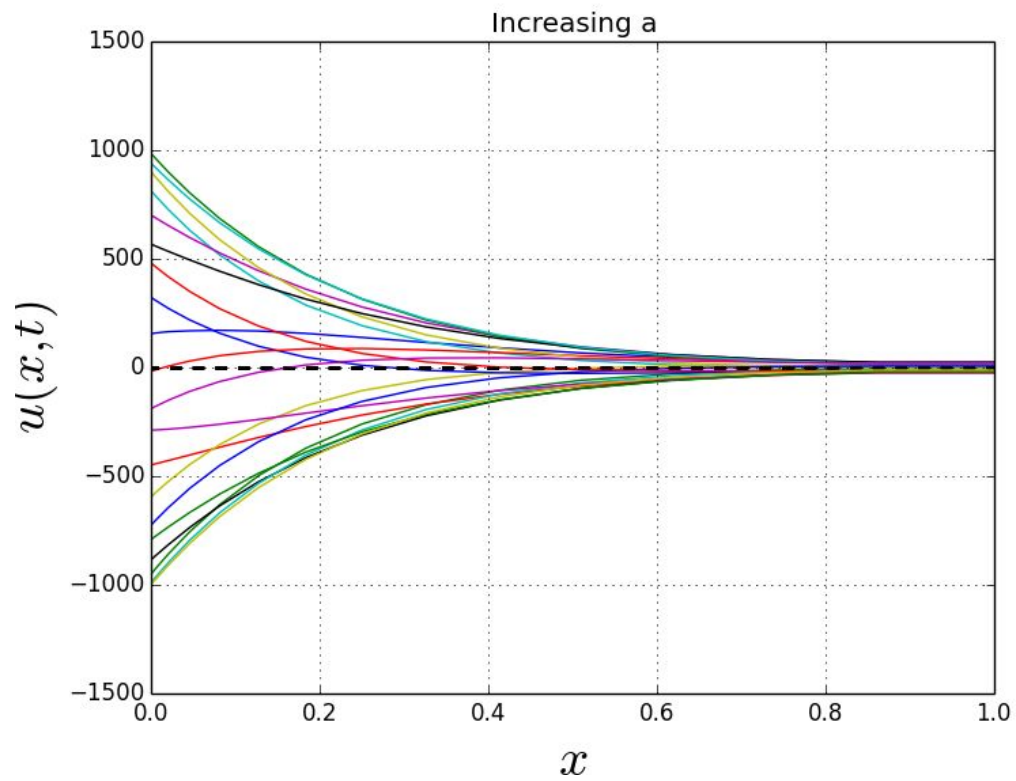


Figure 19. Steady-state solution with increasing a

With a increases, the amplitude of boundary condition on the left side is increased which will result in the boundary layer much thicker.

(b)

$$\delta = f(c, \alpha, \beta, L_x, a, \omega)$$

$$\Rightarrow f(\delta, c, \alpha, \beta, L_x, a, \omega) = 0$$

number of variables: 7

number of dimensions: 2 (length L and time T)

number of π groups: $7 - 2 = 5$.

δ	L		δ	L		$\frac{\delta}{L_x}$	1	
C	$\frac{L}{T}$		$\frac{C}{\omega}$	L		$\frac{C}{\omega L_x}$	1	
α	$\frac{L^2}{T}$	$\xrightarrow{\text{Cancel T}}$	$\frac{\alpha}{\omega}$	L^2	$\xrightarrow{\text{Cancel L}}$	$\frac{\alpha}{\omega L_x^2}$	1	} 5 π groups
β	$\frac{1}{T}$		$\frac{\beta}{\omega}$	1		$\frac{\beta}{\omega}$	1	
L_x	L	L_x	L					
a	$\frac{L}{T}$	$\frac{a}{\omega}$	L		$\frac{a}{\omega L_x}$	1		
ω	$\frac{1}{T}$							

$$\text{So. } f\left(\frac{\delta}{L_x}, \frac{C}{\omega L_x}, \frac{\alpha}{\omega L_x^2}, \frac{\beta}{\omega}, \frac{a}{\omega L_x}\right) = 0$$

$\downarrow \quad \downarrow \quad \downarrow \quad \downarrow \quad \downarrow$
 $\pi_1 \quad \pi_2 \quad \pi_3 \quad \pi_4 \quad \pi_5$

$$\Rightarrow \frac{\delta}{L_x} = f(\pi_2, \pi_3, \pi_4, \pi_5)$$
$$= f\left(\frac{C}{\omega L_x}, \frac{\alpha}{\omega L_x^2}, \frac{\beta}{\omega}, \frac{a}{\omega L_x}\right)$$

In order to verify the derived scaling laws. What we need to do is to vary L_x and keep π groups on the right-hand to be constant. In this way, other parameters might be varied to

keep each pi groups to be constant. Plot the boundary layer thickness against L_x , this should be a straight line.

The result is shown below:

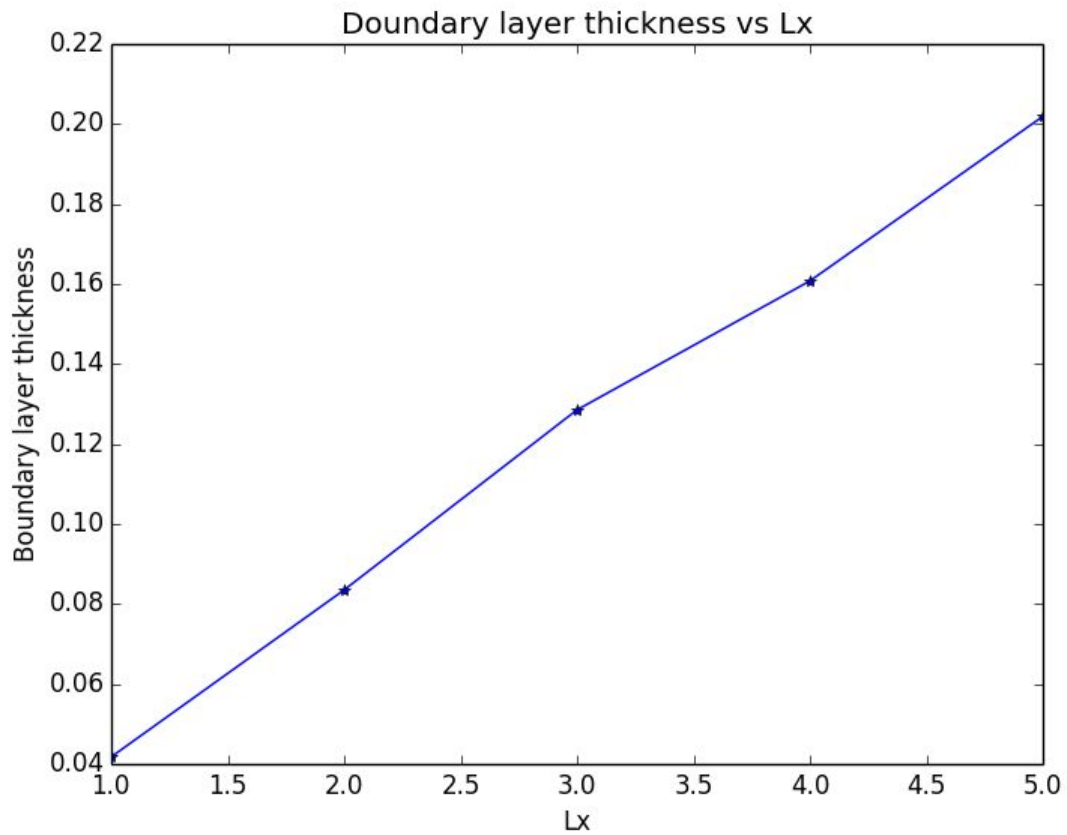


Figure 20. Boundary layer thickness vs L_x

From the plot, the relationship between boundary layer thickness and L_x is linear and with positive slope. This result verifies the scaling laws derived from pi theorem.